Further Encounters with Clear Air Turbulence in Research Aircraft

P. J. KENNEDY AND M. A. SHAPIRO

National Center for Atmospheric Research,[1] Boulder, CO 80307

(Manuscript received 24 July 1979, in final form 10 December 1979)

ABSTRACT

A series of aircraft penetrations into clear air turbulence zones within upper level fronts is presented. Heat and momentum diffusivities are estimated with a view toward obtaining more realistic parameterizations for numerical models. Two passes through severe turbulence are discussed in detail.

1. Introduction

The observed energetics of clear air turbulence has been increasingly unraveled with the advent of well-instrumented research aircraft. Researchers have shown that it is possible to delineate quantitatively the components of turbulence energy. For example, Dutton (1969) and Kennedy and Shapiro (1975) computed and accounted for the various terms in the turbulence energy budget. In the course of our continued work on the many aspects of frontal zone-jet stream structure (see Shapiro, 1976, 1978), we have endured several more encounters with clear air turbulence and in this paper we present some of them. One event in particular on 11 April 1978 will be analyzed in detail.

2. The equations

In analyzing a patch of clear air turbulence we use the same terminology and assumptions as in our previous paper on this topic (Kennedy and Shapiro, 1975). For the physical interpretation of the following arguments we suggest the reader see that paper.

Assuming nondivergent motion, horizontal homogeneity and a zero mean vertical velocity, we can

[1] The National Center for Atmospheric Research is sponsored by the National Science Foundation.

TABLE 1. Eddy diffusivity and Richardson number computations for several aircraft penetrations of turbulent zones.

Date	Level (mb)	$\langle vw \rangle$ ($m^2\ s^{-2}$)	$\partial V/\partial z$ (s^{-1})	$\langle w\theta' \rangle$ (m s^{-1} K)	$\partial\theta/\partial z$ (K m^{-1})	K_M ($m^2\ s^{-1}$)	K_H ($m^2\ s^{-1}$)	Pr $= K_M/K_H$	Ri	Rf = Ri/Pr	ϵ ($10^{-2}\ m^2\ s^{-3}$)
19 April 71	470	−1.10	0.017	−0.22	0.003	65	73	0.9	0.35	0.38	1.0
19 April 71	420	−1.50	0.017	−0.15	0.003	88	50	1.8	0.35	0.18	1.7
15 April 76	265	+0.35	−0.017	−0.15	0.011	21	13	1.6	1.12	0.70	0.01
15 April 76	432	−0.51	0.028	−0.12	0.011	18	11	1.6	0.45	0.28	0.00
16 April 76	393	−0.47	0.015	−0.04	0.006	31	7	4.4	0.83	0.19	0.58
16 April 76	217	−0.19	0.018	−0.05	0.022	11	2	5.5	1.96	0.36	0.23
11 April 78	407	−3.50	0.028	−0.89	0.008	146	111	1.3	0.30	0.23	3.17
11 April 78	358	−4.10	0.028	−0.53	0.008	152	66	2.3	0.30	0.13	2.50
Averages						67	42	2.4	0.71	0.31	

Note: The two 11 April 78 cases include the crosswind component, i.e.,

$$K_M = -\frac{\langle vw \rangle(\partial V/\partial z) + \langle uw \rangle(\partial U/\partial z)}{(\partial V/\partial z)^2 + (\partial U/\partial z)^2},$$

$$\mathrm{Ri} = \frac{(g/\theta_0)(\partial\theta/\partial z)}{(\partial V/\partial z)^2 + (\partial U/\partial z)^2},$$

$$\mathrm{Rf} = \frac{(g/\theta_0)\langle w\theta' \rangle}{\langle vw \rangle \partial V/\partial z + \langle uw \rangle \partial U/\partial z}.$$

0022-4928/80/050986-08$06.00

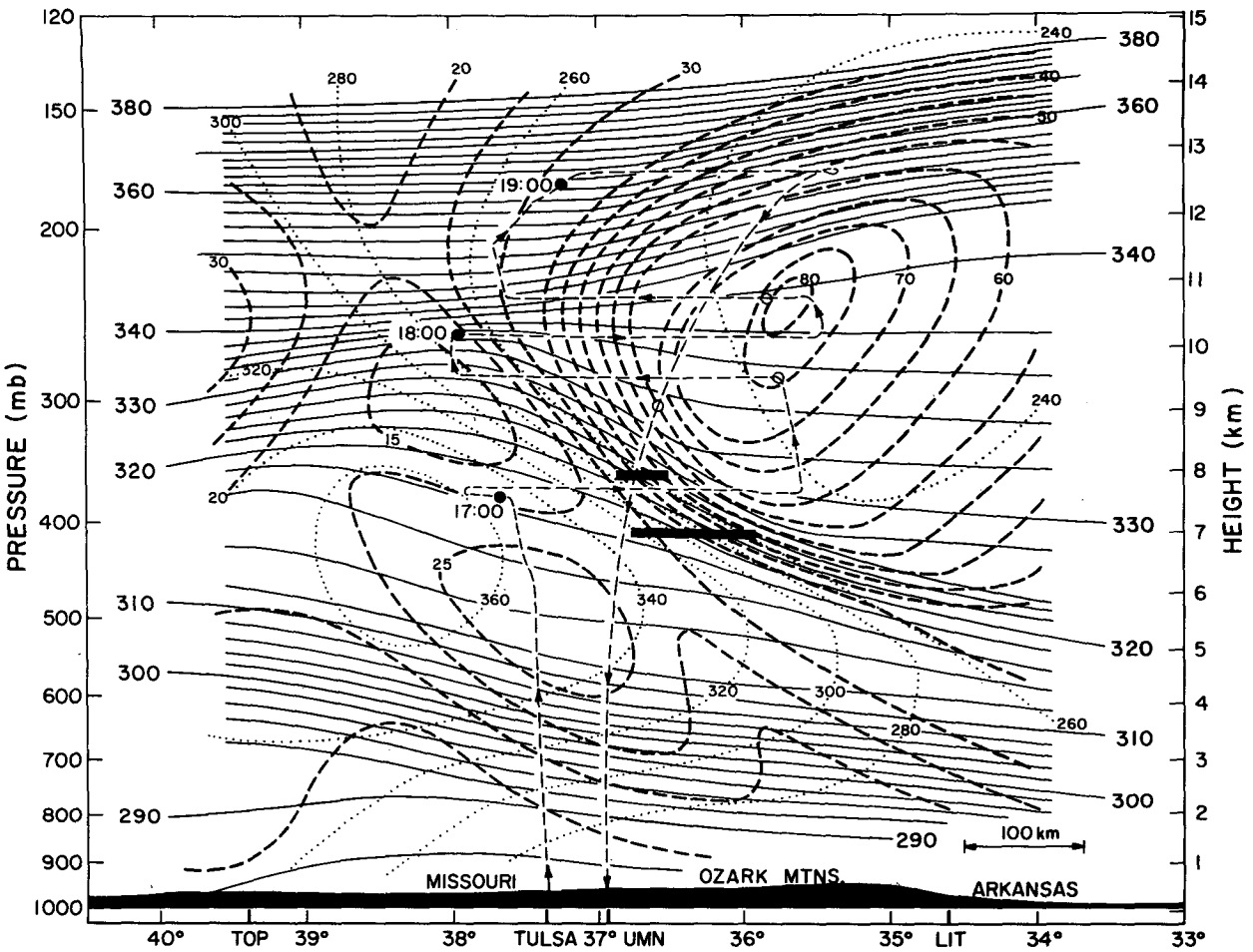

FIG. 1. Cross section of potential temperature (K, solid line), wind speed (m s^{-1}, dashed line) and wind direction (deg, dotted line), 11 April 1978. Flight track indicated with arrowed dashed line. Solid circles indicate hours GMT, open circles half-hours. NWS balloon soundings from Topeka (TOP), Monett (UMN) and Little Rock (LIT) aided in this analysis. The two heavy solid line segments represent the turbulent passes discussed in Section 4.

write the turbulence energy equation as

$$\frac{\partial\langle E\rangle}{\partial t} = -\langle uw\rangle\frac{\partial U}{\partial z} - \langle vw\rangle\frac{\partial V}{\partial z} + \frac{g}{\theta_0}\langle w\theta'\rangle - \epsilon - \frac{\partial}{\partial z}\left(\frac{1}{\rho_0}\langle p'w\rangle + \langle wE\rangle\right). \quad (1)$$

The angle braces indicate an average over space. The lower case u, v and w are perturbations from the mean flow U and V. The specific turbulent kinetic energy is $E = (u^2 + v^2 + w^2)/2$. The quantities θ' and θ_0 are the perturbation and mean potential temperatures; p' and ρ_0 represent the perturbation pressure and the mean density, respectively. The rate of viscous dissipation is ϵ.

If we orient the axes such that the principal component of flow is V, then in our jet stream cases U and $\partial U/\partial z$ become at least an order of magnitude smaller than V and $\partial V/\partial z$. If we also assume that the vertical transport of energy by the turbulence itself is small (see Dutton, 1969), we can rewrite (1) as

$$\frac{\partial\langle E\rangle}{\partial t} = -\langle vw\rangle\frac{\partial V}{\partial z} + \frac{g}{\theta_0}\langle w\theta'\rangle - \epsilon. \quad (2)$$

3. Eddy diffusivities

Before we attempt to balance (2) with observed data, we divert our attention briefly to a discussion of the eddy diffusivities for momentum and heat, K_M and K_H, where

$$K_M = -\frac{\langle vw\rangle}{\partial V/\partial z} \quad \text{and} \quad K_H = -\frac{\langle w\theta'\rangle}{\partial\theta/\partial z}. \quad (3)$$

Most experimental values of K_M and K_H have been calculated in the boundary layer. Two exceptions

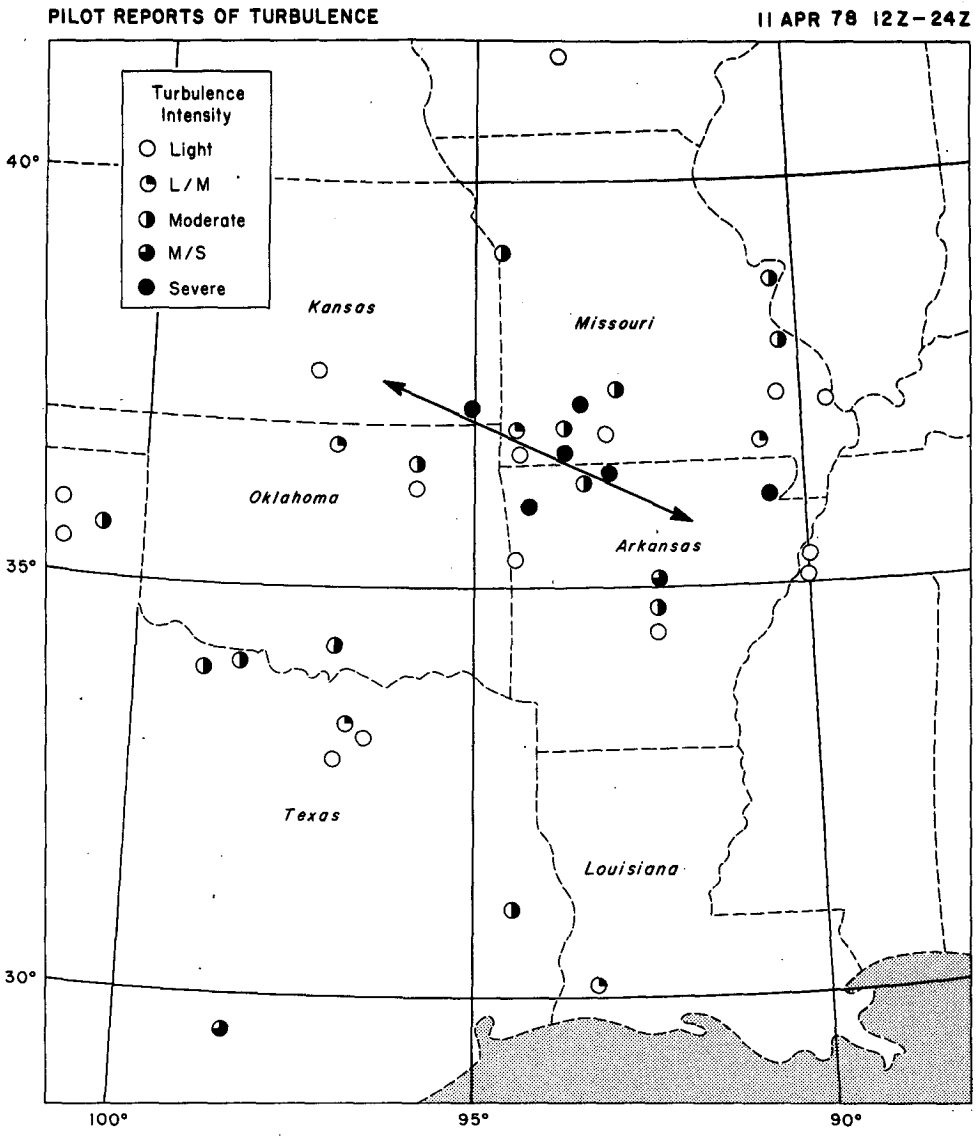

FIG. 2. Pilot reports of turbulence and chop in an area of central United States from 1200 to 2400 GMT 11 April 1978. The approximate tracks of the Sabreliner during its research flight on this day are represented by the oblique line near the center.

are the observations by Lilly *et al.* (1974) of stratospheric turbulence and by Lilly (1978) of mountain-induced mid-tropospheric turbulence. Both studies used aircraft as the primary observing platform, the former having summarized 24 000 flight kilometers of turbulence. In the boundary layer, we have, for example, the 1968 Kansas Field Program where the Air Force Cambridge Research Laboratories computed tables of diffusivity values, which later Businger *et al.* (1971) condensed into useful diagrams. Since mixing-length theory and the parameterization of momentum and heat flux using K_M and K_H are used in numerical modeling of frontal activity as well as the atmospheric boundary layer, we thought it useful to compile a table of diffusivities observed in some moderate-to-severe patches of turbulence within fronts.

In Table 1 we show eight examples. The covariances $\langle vw \rangle$ and $\langle w\theta' \rangle$ are straightforward calculations after first removing means and linear trends from the original time series. While we are confident in these covariance calculations, there is some arguable latitude in the estimate of the vertical gradients of V and θ. Also the question arises: how

TABLE 2. Energy budget computation for Sabreliner penetration of a turbulent zone, 11 April 1978.

	Altitude	
	407 mb	358 mb
ENERGY PRODUCTION		
Shear		
$\partial V/\partial z$	2.75×10^{-2} s^{-1}	2.75×10^{-2} s^{-1}
$\partial U/\partial z$	0.75×10^{-2} s^{-1}	0.75×10^{-2} s^{-1}
$\partial V/\partial x$	-0.04×10^{-2} s^{-1}	-0.04×10^{-2} s^{-1}
Reynolds stress		
$\langle vw \rangle$	-3.50 m^2 s^{-2}	-4.10 m^2 s^{-2}
$\langle uw \rangle$	-3.02 m^2 s^{-2}	-1.43 m^2 s^{-2}
$\langle uv \rangle$	6.80 m^2 s^{-2}	0.11 m^2 s^{-2}
Total production		
$-\langle vw \rangle \partial V/\partial z$	9.63×10^{-2} m^2 s^{-3}	11.28×10^{-2} m^2 s^{-3}
$-\langle uw \rangle \partial U/\partial z$	2.27×10^{-2} m^2 s^{-3}	1.07×10^{-2} m^2 s^{-3}
$-\langle uv \rangle \partial V/\partial x$	0.27×10^{-2} m^2 s^{-3}	0.00
Sum	12.17×10^{-2} m^2 s^{-3}	12.35×10^{-2} m^2 s^{-3}
ENERGY LOSSES		
Temperature flux		
$\langle w\theta' \rangle$	-0.89 m s^{-1} K	-0.53 m s^{-1} K
Buoyancy		
$(g/\theta_0)\langle w\theta' \rangle$	-2.69×10^{-2} m^2 s^{-3}	-1.59×10^{-2} m^2 s^{-3}
Frictional dissipation		
$-\epsilon$	-3.17×10^{-2} m^2 s^{-3}	-2.50×10^{-2} m^2 s^{-3}
Total losses		
$(g/\theta_0)\langle w\theta' \rangle - \epsilon$	-5.86×10^{-2} m^2 s^{-3}	-4.09×10^{-2} m^2 s^{-3}
RESIDUAL		
	6.31×10^{-2} m^2 s^{-3}	8.26×10^{-2} m^2 s^{-3}
ADDITIONAL QUANTITIES		
Stability		
$(g/\theta_0)(\partial\theta/\partial z)$	2.4×10^{-4} s^{-2}	2.4×10^{-4} s^{-2}
Richardson number		
$\dfrac{(g/\theta_0)(\partial\theta/\partial z)}{(\partial V/\partial z)^2 + (\partial U/\partial z)^2}$	0.30	0.30
Flux Richardson number		
$\dfrac{(g/\theta_0)\langle w\theta' \rangle}{\langle vw \rangle \partial V/\partial z + \langle uw \rangle \partial U/\partial z}$	0.23	0.13
Variances		
$\langle \theta'^2 \rangle$	0.67 K^2	0.43 K^2
$\langle v^2 \rangle$	12.4 m^2 s^{-2}	13.6 m^2 s^{-2}
$\langle u^2 \rangle$	15.4 m^2 s^{-2}	9.1 m^2 s^{-2}
$\langle w^2 \rangle$	7.3 m^2 s^{-2}	4.9 m^2 s^{-2}

representative are our passes through these turbulence zones? Each of the estimates of $\partial V/\partial z$ and $\partial\theta/\partial z$, however, comes from inspecting the vertical cross section on the given flight day, which was drawn and interpolated using the full complement of flight legs at different levels, plus aircraft and National Weather Service (NWS) balloon soundings. An example of such a cross section is presented in Fig. 1. The differential Δz used in obtaining $\partial V/\partial z$ and $\partial\theta/\partial z$ is of order 0.5 km, which is smaller than the vertical extent of the shear layers (~1 km). Such a differential is crude, but the ideal of flying simultaneously a vertically stacked armada of intercalibrated research aircraft at, say, 100 m vertical spacing is cost-prohibitive, if not dangerous.

Two of the eight examples (19 April 1971) in Table 1 are taken from our 1975 paper. The other six represent new data. Despite the wide range in K_M,

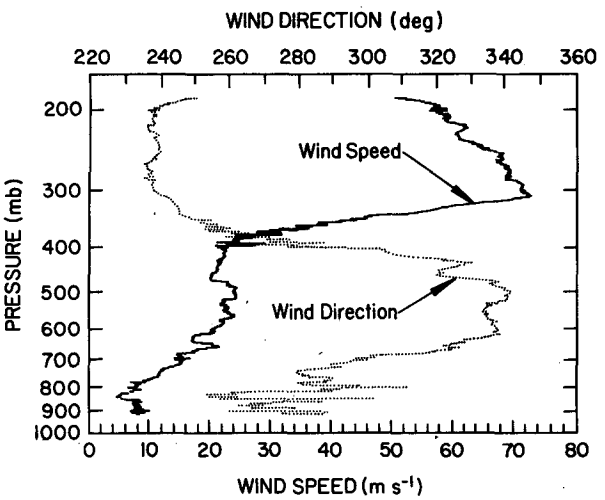

FIG. 3. Sabreliner sounding of wind speed and direction through frontal zone, 11 April 1978. The long descent in the flight track on Fig. 1 (center) shows the location and time.

K_H and ϵ, we do see that the Prandtl number, Pr $= K_M/K_H$, is a little more consistent from case to case, although its average value of 2.4 is higher than the typical values of 0.5–1.0 found in the atmospheric boundary layer (see Businger *et al.*, 1971).

One should not blindly accept these fairly large calculated Prandtl numbers. Although we are not aware of any general theoretical result that clearly rejects eddy Prandtl numbers greater than unity, the preponderance of boundary-layer observations is fairly convincing evidence of Pr $\approx$ 1. The nature of turbulence in a stably stratified flow is such that the vertical scales tend to be suppressed, and the flow is substantially unaware of its lower boundary condition. Thus there should be no essential difference between shear-driven, statically stable boundary-layer turbulence and that at higher levels, except for the length and velocity scales imposed by the shear layer. It is not unreasonable to assume that the local wind shear in our selected patches of turbulence could have been twice that shown in Table 1, resulting in Pr values closer to unity. Again, one airplane and a nearby NWS balloon sounding are not optimal platforms for measuring that crucial, instantaneous $\partial V/\partial z$.

The columns of Richardson number Ri and flux Richardson number Rf shed some light on the accuracy of the vertical wind shear measurements. One would expect Ri to be nearer to the critical 0.25 than our average of 0.71. The implication, again, is an underestimation of $\partial V/\partial z$.

The theory of the inertial subrange (see Chaps. 2.9 and 5.2, Lumley and Panofsky, 1964) is used in calculating the dissipation rate ϵ shown in the last column of Table 1. In the turbulent patch, if the power spectral density of a velocity component falls off with the $-5/3$ power of wavenumber, one can get an estimate of ϵ by solving

$$S(k) = A\epsilon^{2/3}k^{-5/3}, \tag{4}$$

where S is the power spectral density, k the wavenumber expressed in radians per unit length, and A is a constant equal to ~0.5 for longitudinal (along flight track) perturbations and ~0.67 for lateral and vertical perturbations (Gibson *et al.*, 1970). In all eight examples of Table 1, the $-5/3$ power law is evident for all three velocity components, although our data frequency cutoff of 1 Hz (~300 m) leaves some room for error in these dissipation estimates. We solved (4) by simply extending a $-5/3$ slope line drawn through the spectrum on a log-log plot to the point where $k = 1$ and then reading the associated $S(k)$, i.e., $\epsilon = [S(1)/A]^{3/2}$. For each of the eight cases, we performed this graphic estimation for each of the three velocity components and then averaged the ϵ so obtained.

4. The 11 April 1978 case

The 11 April 1978 event provided our most intense encounter with clear air turbulence to date. In addition, there were numerous reports (see Fig. 2) of moderate and severe turbulence and chop from commercial aircraft in this area of southwest Missouri and northwest Arkansas. Our flight plus other Spring 1978 data will be analyzed from a more thorough and synoptic viewpoint in future publications, but we do show here (Fig. 1) a vertical cross section of the temperature and wind for reference. It is a composite of NWS balloon soundings and our own Sabreliner data. The two turbulence passes at 407 and 358 mb are shown as heavy solid line segments; they do not appear as part of the flight track proper because they occurred during a second research flight two hours after the time of this cross section.

The magnitudes of the covariances and dissipation are quite large and we found it enlightening to "balance" the simplified turbulent energy equation (2). In an event of this intensity it is questionable that an accurate or representative measurement of wind shear and temperature gradient can be made or that $\partial\langle E\rangle/\partial t$ is near zero. Indeed, all assumptions made in obtaining (1) or (2) must be held suspect.

In Table 2 we show the components of the turbulent energy equation. We have oriented our axes such that V is the principal component of the total wind: 280° for the 407 mb leg and 262° for the 358 mb leg. In both legs the direction of U is defined

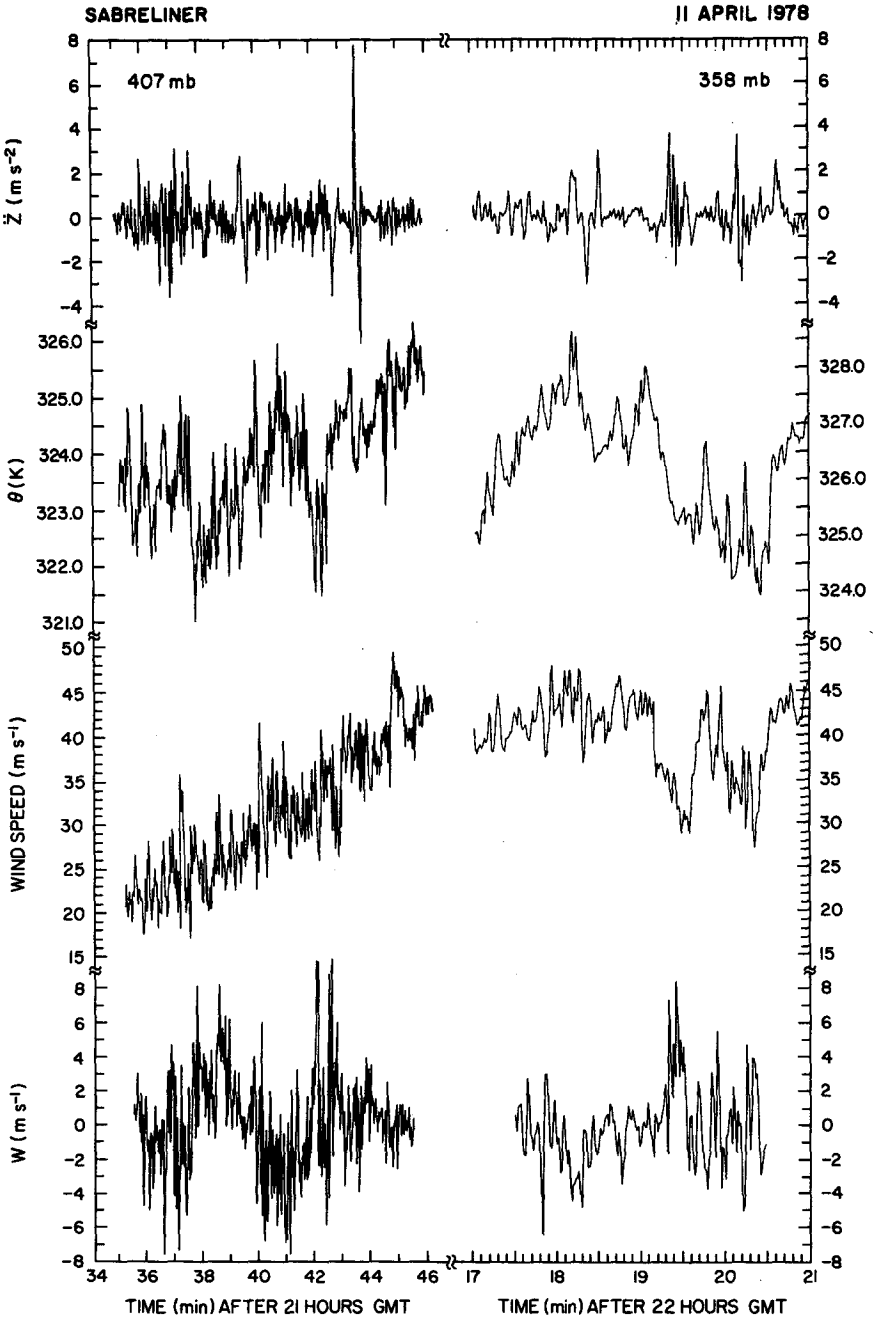

FIG. 4. Time series plots of vertical airplane acceleration, potential temperature, horizontal and vertical wind speeds for the 407 and 358 mb passes through clear air turbulence, 11 April 1978.

as the direction of V minus 90°. We have included three of the $\langle u_i u_j \rangle \partial U_i/\partial x_j$ Reynolds stress terms nonetheless, since contributions to energy production other than $\langle vw \rangle \partial V/\partial z$ rise above the noise level in this case.

In the energy production columns, the Reynolds stresses are large and are acting strongly to destroy the large vertical wind shear, which is shown in the Fig. 3 Sabreliner sounding. The $\langle vw \rangle$ stress corresponds to a vertical flux of horizontal momentum of $\sim$20 dyn cm^{-2}.

In the energy loss columns, we find an enormous

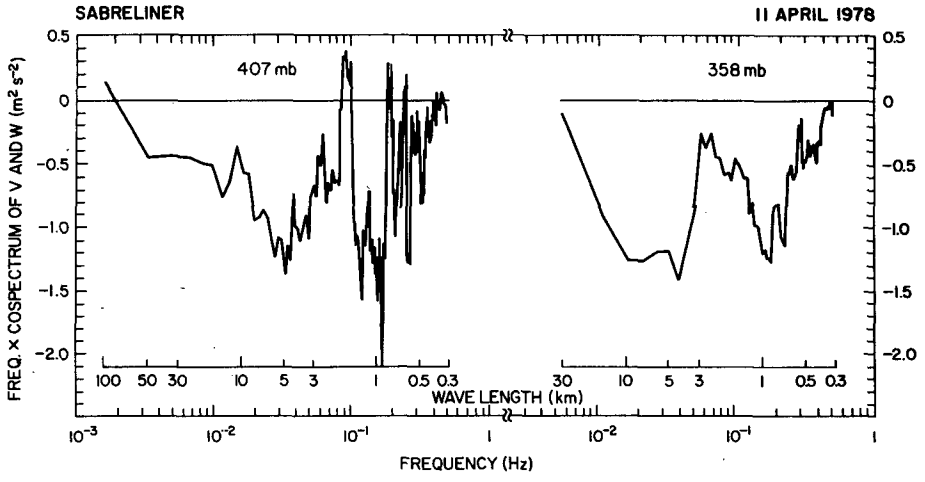

FIG. 5. Cospectra of horizontal and vertical wind for the 407 and 358 mb passes through clear-air turbulence, 11 April 1978. Ordinate is multiplied by frequency to render a variance area-conserving plot.

heat flux for a CAT case: a covariance of w and θ' of 0.5–1.0 m s^{-1} K. As a point of reference, Shapiro (1976, 1978) used a $\langle w\theta' \rangle \approx 0.15$–$0.20$ m s^{-1} K (thought to be large at the time) in his estimation of potential vorticity changes in fronts. The frictional dissipation rate $\epsilon \approx 3 \times 10^{-2}$ m^2 s^{-3} (or 300 cm^2 s^{-3}) corresponds "objectively" to moderate-to-severe turbulence. However, there is probably no unique, objective relationship between ϵ and severity of turbulence since speed and type of aircraft, for example, are unaccounted variables. In these two passes, we do know that the pilots and observer (Shapiro) logged "severe turbulence."

Table 2 clearly shows a poor balance of the energy production and loss terms: the residual is as large as the components. But, as we have noted, the simplified equation plus the uncertainty of shear measurements in severe CAT make accurate analysis somewhat difficult.

We show the time series of horizontal and vertical wind speed, potential temperature and vertical aircraft acceleration in Fig. 4. The turbulent character of these two passes is apparent, especially considering that these data are 1 s *averages*. If we look at some of the data in Fourier space (Figs. 5 and 6), we can see that the large negative covariances $\langle vw \rangle$ and $\langle w\theta' \rangle$ arise from virtually every wavenumber contributing.

The spectral analysis technique deserves a few words here. A fast Fourier transform was used on the time series with means and linear trends removed initially and the first and last 10% of the

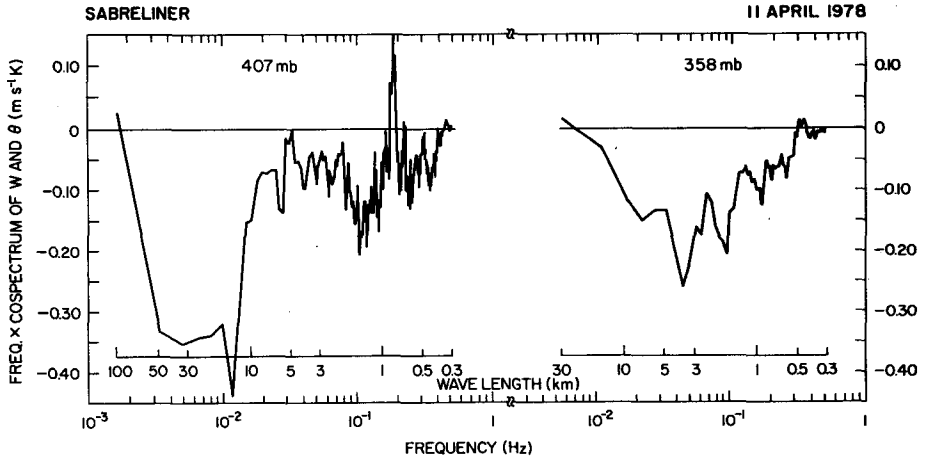

FIG. 6. As in Fig. 5 except for vertical wind and potential temperature.

series tapered with a cosine weighting. To produce a smoother plot, each of the points on the spectral curves is a centered average of the adjacent eleven spectral estimates, except at either end where 1-, 3-, 5-, 7- and 9-point averages are taken. Note that the vertical axis has been multiplied by frequency to produce a plot in which area is proportional to the covariance. Assuming that the turbulent features are embedded in the mean flow and not tied to the topography beneath, we computed the wavelength axis shown, by simply dividing the true air speed by the frequency.

5. Conclusions

With instrumented research aircraft and a careful flight profile, it is possible to compute approximate exchange coefficients for heat and momentum in clear-air turbulence zones associated with fronts. The directly measured values of K_M and K_H should prove useful to numerical modelers of frontogenesis. As an example, Gidel and Shapiro (1979) utilized a range of Prandtl numbers and exchange coefficients from the present study in a parameterization of turbulent heat and momentum fluxes within a two-dimensional isentropic-coordinate primitive equation model of jet stream circulations and tropopause folding.

Our observed large Prandtl numbers should be accepted with reservation, since accurate measurement of vertical gradients is difficult in turbulent zones. Typical Prandtl numbers for planetary boundary layer turbulence are near unity. Therefore, it remains for future research to provide additional quantitative measurements of CAT to clearly establish the representativeness of the Prandtl numbers found from the limited number of cases presented in this study. Future work is also required on the *theoretical* aspects of turbulent mixing processes to address this question: does vertical mixing by motions on scales ~1 to 20 km within the strong thermally stratified frontal shear layers possess characteristic Prandtl numbers significantly larger than those of the smaller scale (<1 km) mixing motions within the planetary boundary layer?

Regarding the balancing of the turbulent energy equation, we found that, in our two passes through severe turbulence, calculations show very large eddy diffusivities but also an imbalance of terms due probably to non-steady-state, uncertain vertical shears, and possible pressure torque contributions.

Acknowledgments. The authors are grateful to Dr. D. K. Lilly and two anonymous reviewers for their thoughtful comments and suggestions.

REFERENCES

Businger, J. A., J. C. Wyngaard, Y. Izumi and E. F. Bradley, 1971: Flux-profile relationships in the atmospheric surface layer. *J. Atmos. Sci.*, **28,** 181–189.

Dutton, J. A., 1969: An energy budget for a layer of statospheric CAT. *Radio Sci.*, **4,** 1137–1142.

Gibson, C. H., G. R. Stegen and R. B. Williams, 1970: Statistics of the finestructure of turbulent velocity and temperature fields measured at high Reynolds number. *J. Fluid Mech.*, **41,** 153–167.

Gidel, L. T., and M. A. Shapiro, 1979: The role of clear air turbulence in the production of potential vorticity in the vicinity of upper tropospheric jet stream-frontal systems. *J. Atmos. Sci.*, **36,** 2125–2138.

Kennedy, P. J., and M. A. Shapiro, 1975: The energy budget in a clear air turbulence zone as observed by aircraft. *Mon. Wea. Rev.*, **103,** 650–654.

Lilly, D. K., 1978: A severe downslope windstorm and aircraft turbulence event induced by a mountain wave. *J. Atmos. Sci.*, **35,** 59–77.

——, D. E. Waco and S. I. Adelfang, 1974: Stratospheric mixing estimated from high-altitude turbulence measurements. *J. Appl. Meteor.*, **13,** 488–493.

Lumley, J. L., and H. A. Panofsky, 1964: *The Structure of Atmospheric Turbulence.* Interscience, 239 pp.

Shapiro, M. A., 1976: The role of turbulent heat flux in the generation of potential vorticity in the vicinity of upper level jet stream systems. *Mon. Wea. Rev.*, **104,** 892–906.

——, 1978: Further evidence of the mesoscale and turbulent structure of upper level jet stream-frontal zone systems. *Mon. Wea. Rev.*, **106,** 1100–1111.